Two Types of Sources of Wave Trains in a Two-Variable Chemical Model of a Bistable Reaction−Diffusion System

Marcin Leda and Andrzej L. Kawczyński*

Institute of Physical Chemistry, Polish Academy of Sciences, Warsaw, Poland

Received: May 4, 2004; In Final Form: July 23, 2004

A realistic 1D model of a bistable two-variable chemical system with a stable focus (SF) surrounded by a stable limit cycle (SLC) is investigated. Initial excitations of a subinterval of the system can generate two types of wave sources depending on the value of the bifurcation parameter which determines the basin of attraction of SF. For a sufficiently small basin of attraction of SF, an initial local excitation of a finite system generates a finite sequence of traveling impulses. Each subsequent impulse is wider than the previous one, and this is the reason finite sequences of impulses can be observed in finite systems. In infinite systems, an infinite number of impulses is generated. If the basin of attraction of SF is sufficiently large, another type of wave source is induced by the initial excitation. Traveling impulses of excitation have a local minimum between their front and back. The wave source generates an infinite number of impulses both in finite systems and in infinite ones.

1. Introduction

Target patterns (trains of circular impulses) in chemical systems were observed for the first time in 1970 by Zaikin and Zhabotinsky.[1] In a thin layer of a solution containing appropriate concentrations of bromate, bromomalonic acid, ferroine, and sulfuric acid, concentric blue rings (high concentration of the oxidized form of ferroine) spread from a few wave sources, which oscillate with greater frequency than the rest of the medium. The wave sources appear spontaneously. However, they can also be generated by local excitations of the unexcited (red) area, for example, by taking a small drop from an excited blue ring and transferring it to an unexcited region.[2] Target patterns were subsequently observed in many variations of the Belousov−Zhabotinsky (B−Z) reaction,[3,4] in uncatalyzed bromate oscillators[5] and in chlorite−iodide oscillators.[6] They also appear in heterogeneous systems at the oscillatory oxidation of carbon monoxide on a platinum surface.[7]

Two kinds of explanations of the creation of target patterns are known in the literature. One of them is based on the assumption that some heterogeneities (pacemakers) exist in the reaction mixture or on the Petri dish. Small impurities in the reaction mixtures or scratches on the surface of the Petri dish can play the role of pacemakers. By definition, the system oscillates with higher frequency at pacemakers than in their homogeneous neighborhood. Each pacemaker excites its neighborhood and forces the system to oscillate with its own frequency. In this case, the reaction−diffusion equations[8,9] contain kinetic terms which depend explicitly on the place where the pacemakers are localized.

The other explanation is based on the assumption that wave sources (leading centers) appear in systems without heterogeneities. A local increase of oscillation frequency is induced by local excitation and is entirely generated by chemical dynamics itself. Appropriate local excitations may appear due to internal fluctuations. In the deterministic description of leading centers, initial conditions play the role of local excitations. The reaction−diffusion equations contain kinetic terms which do not depend explicitly on the spatial coordinates and are the same in the whole system.[9,10]

Experimental observations[2] with artificial heterogeneities and transferring a drop of the solution from the excited to the unexcited region corroborate the possibility of both types of wave sources in the B−Z system. It is noteworthy that known models of leading centers in excitable or oscillatory systems consist of at least three or more variables.[9,10]

In this paper, we present a two-variable model of wave sources in a one-dimensional (1D) system. The model does not contain any heterogeneous terms with explicit dependence on the space coordinate. The idea of the model is based on the coexistence of a stable steady state and a stable limit cycle above the subcritical Hopf bifurcation. In the model, two different types of sustained wave sources can appear. It should be stressed that the wave sources described in the present paper have different features than the target patterns observed in the experiments as well as in the models known so far. In particular, they have nearly the same frequency of generation of impulses as the frequency of stable limit cycle oscillations.

In the next section, we describe a reasonable chemical scheme, whose dynamics is reduced to two variables and exhibits the subcritical Hopf bifurcation. The properties of two types of sustained wave sources and two types of impulses of excitation spreading from them are then described. The role of the initial conditions in the formation of the sources and interactions between them are discussed. The last section contains the discussion and suggestions for experiments in real chemical systems.

2. Model

Let us consider the following scheme of elementary reactions (mono- or bimolecular reactions without autocatalysis):

* Corresponding author. E-mail: alk@ichf.edu.pl.

10.1021/jp0480899 CCC: $27.50
Published on Web 08/26/2004

$$S_0 \underset{k_{-1}}{\overset{k_1}{\rightleftharpoons}} S \quad (1)$$

$$S_0 + E \underset{k_{-2}}{\overset{k_2}{\rightleftharpoons}} SE \quad (2)$$

$$SE \xrightarrow{k_3} E + P \quad (3)$$

$$S + SE \underset{k_{-4}}{\overset{k_4}{\rightleftharpoons}} S_2E \quad (4)$$

$$P + E \underset{k_{-5}}{\overset{k_5}{\rightleftharpoons}} EP \quad (5)$$

$$SE + P \underset{k_{-5}}{\overset{k_5}{\rightleftharpoons}} SEP \quad (6)$$

$$S_2E + P \underset{k_{-5}}{\overset{k_5}{\rightleftharpoons}} S_2EP \quad (7)$$

$$P + E' \underset{k_{-6}}{\overset{k_6}{\rightleftharpoons}} PE' \quad (8)$$

$$PE' \xrightarrow{k_7} E' + R \quad (9)$$

where S_2E, EP, SEP, and S_2EP are nonactive complexes of the catalyst (enzyme) E. Throughout the paper, capital letters denote reagents and their concentrations as well, because this notation does not introduce misunderstandings.

The model is based on two coupled catalytic (enzymatic) reactions described by the Langmuir−Hinshelwood (Michaelis−Menten) scheme. The first reaction is inhibited by an excess of its reactant S and product P. We take the identical rate constants for reactions 5−7, which is a reasonable assumption if the inhibition by the product P has an allosteric character. The product of the first reaction is the reactant for the next one. The system is open to the reactant and to the product due to the first and the last two reactions in the above scheme.

Note that the total concentrations of both catalysts remain constant. This allows us to eliminate the concentrations of the complexes SE and PE' from the dynamics of the system, which can be described by the following eight kinetic equations for dimensionless variables:

$$\frac{ds}{dt} = \frac{k_1 S_0}{k_3 E_0} - \frac{k_{-1} K_m}{k_3 E_0} s + \frac{k_{-2}}{k_3}(1 - e - s_2e - sep - s_2ep - ep) - \frac{k_2}{k_3} K_m e\cdot s - \frac{k_4}{k_3} K_m s(1 - e - s_2e - sep - s_2ep - ep) + \frac{k_{-4}}{k_3} s_2e = f_1(s,e,s_2e,sep,s_2ep,ep) \quad (10a)$$

$$\frac{dp}{dt} = b\left\{1 - e - s_2e - sep - s_2ep - ep - \frac{k_{-5}}{k_3}(p\cdot e - ep) - \frac{k_{-5}}{k_3}[p(1 - e - s_2e - sep - s_2ep - ep) - sep] - \frac{k_{-5}}{k_3}(p\cdot s_2e - s_2ep) + \left[\frac{k_{-6}}{k_3}(1 - e') - \frac{k_6}{K_5 k_3} p\cdot e'\right]\frac{E_0'}{E_0}\right\} = f_2(p,e,s_2e,sep,s_2ep,ep,e') \quad (10b)$$

$$\frac{de}{dt} = \frac{1}{\epsilon}\left\{\frac{k_{-2}}{k_3}(1 - e - s_2e - sep - s_2ep - ep) - \frac{k_2}{k_3} K_m e\cdot s - \frac{k_{-5}}{k_3}(p\cdot e - ep) + 1 - e - s_2e - sep - s_2ep - ep\right\} = \frac{1}{\epsilon} g_1(s,p,e,s_2e,ep,sep,s_2ep) \quad (10c)$$

$$\frac{ds_2e}{dt} = \frac{1}{\epsilon}\left\{\frac{k_4}{k_3} K_m s(1 - e - s_2e - sep - s_2ep - ep) - \frac{k_{-4}}{k_3} s_2e - \frac{k_{-5}}{k_3}(p\cdot s_2e - s_2ep)\right\} = \frac{1}{\epsilon} g_2(s,p,e,s_2e,sep,s_2ep) \quad (10d)$$

$$\frac{dep}{dt} = \frac{1}{\epsilon}\frac{k_{-5}}{k_3}(p\cdot e - ep) = \frac{1}{\epsilon} g_3(p,e,ep) \quad (10e)$$

$$\frac{dsep}{dt} = \frac{1}{\epsilon}\frac{k_{-5}}{k_3}\{p(1 - e - s_2e - sep - s_2ep - ep) - sep\} = \frac{1}{\epsilon} g_4(p,e,s_2e,sep,s_2ep) \quad (10f)$$

$$\frac{ds_2ep}{dt} = \frac{1}{\epsilon}\frac{k_{-5}}{k_3}(p\cdot s_2e - s_2ep) = \frac{1}{\epsilon} g_5(p,s_2e,s_2ep) \quad (10g)$$

$$\frac{de'}{dt} = \frac{1}{\epsilon}\left\{\frac{k_{-6}}{k_3}(1 - e') - \frac{k_6}{K_5 k_3} p\cdot e' + \frac{k_7}{k_3}(1 - e')\right\} = \frac{1}{\epsilon} g_6(p,e') \quad (10h)$$

where $s = S/K_m$, $p = K_5P$, $e = E/E_0$, $s_2e = S_2E/E_0$, $ep = EP/E_0$, $sep = SEP/E_0$, $s_2ep = S_2EP/E_0$, and $e' = E'/E_0$ are dimensionless concentrations of the reactant S, the product P, the free enzyme E, the nonactive complexes of the enzyme E with the reactant and product, and the free enzyme E', respectively, $t = k_3E_0/K_mt'$ is the dimensionless time (t' is real time), $K_5 = k_5/k_{-5}$, $K_m = (k_{-2} + k_3)/k_2$, and $\epsilon = E_0/K_m$.

We reduce the dynamics described by eq 10 in a rigorous way using the quasi-stationary state approximation. Note that ϵ^{-1} appears as the multiplier in the right-hand sides of eqs 10c−h but not in eqs 10a and b. Moreover, all $g_i(\cdot)$ are linear functions of the arguments e, s_2e, ep, sep, s_2ep, and e'. The solutions to the equations $g_i(\cdot) = 0$ can be written as $\phi_i(s,p)$. For given values of s and p, the solutions to eqs 10c−h have the general form $\psi_i = \psi_{i0}\exp(-t/\epsilon)$. If $\epsilon \to 0$, then according to the Tikhonov theorem,[11] the solutions to eqs 10a−h for time greater than $\tau \sim \epsilon|\ln \epsilon|$ approach the solutions to eqs 10a and b with the values of e, s_2e, ep, sep, s_2ep, and e' given by $\phi_i(s,p)$. We assume that $\epsilon \ll 1$, which is consistent with experimental conditions, because usually total concentrations of catalysts (enzymes) are 10^{-5}−10^{-6}, that is, several orders lower than the concentrations of reactants and products. In a dimensionless time scale, we can describe the dynamics of the system by the equations for the reactant S and the product P in the following form:

$$\frac{ds}{dt} = a_1 - a_2 s - \frac{s}{(1 + s + a_3 s^2)(1 + p)} \quad (11)$$

$$\frac{dp}{dt} = b\left(\frac{s}{(1 + s + a_3 s^2)(1 + p)} - \frac{b_1 p}{b_2 + p}\right) \quad (12)$$

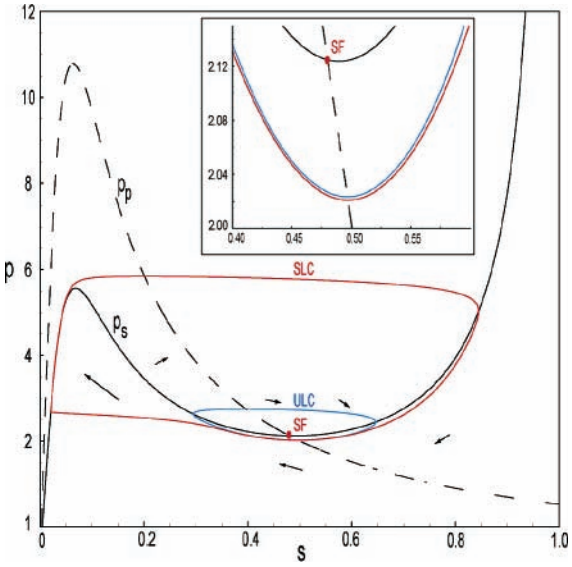

Figure 1. Nullclines of eqs 11 and 13 on the phase plane (s,p) with the stable focus (red), the stable limit cycle (red), and the unstable limit cycle (blue) for $a_1 = a_2 = 0.005$, $a_3 = 250$, $b_1 = 0.0026$, and $b = 0.4$. The arrows schematically show the directions of the vector field.

where $a_1 = k_1S_0/(k_3E_0)$, $a_2 = k_{-1}K_m/(k_3E_0)$, $a_3 = k_4/k_{-4}K_m$, $b = K_mK_5$, $b_1 = k_7E_0'/(k_3E_0)$, $b_2 = K_m'K_5$, and $K_m' = (k_{-6} + k_7)/k_6$. For simplicity, we assume that the reaction with the second catalyst E' occurs in its saturation regime. Then, $p \gg b_2$, and finally,

$$\frac{dp}{dt} = b\left(\frac{s}{(1 + s + a_3s^2)(1 + p)} - b_1\right) \tag{13}$$

The nullclines of eqs 11 and 13 have the following form:

$$p_s = \frac{s}{(1 + s + a_3s^2)(a_1 - a_2s)} - 1 \tag{14}$$

$$p_p = \frac{s}{b_1(1 + s + a_3s^2)} - 1 \tag{15}$$

Note that the nullclines have one intersection point, which corresponds to the stationary state with coordinates (see Figure 1)

$$s_0 = \frac{a_1 - b_1}{a_2} \tag{16}$$

$$p_0 = \frac{s_0}{b_1(1 + s_0 + a_3s_0^2)} - 1 \tag{17}$$

It is easy to check, using the Descartes theorem, that the necessary condition for an N-shaped form of p_s (the existence of two extremes for positive values of s) is $a_1a_3 > a_2$. We assume below such values of a_1, a_2, and a_3 that the nullcline for s is an N-shaped curve on the phase plane (s,p). Moreover, for selected values of the parameters, the stationary state is positioned on the middle (repelling) branch of the nullcline for s, so the stationary state may be unstable.

Note that the parameter b does not change the positions of the nullcline p_p and the stationary state. It only changes the vector field in the direction of the variable p, and therefore, b is the most convenient bifurcation parameter.

It follows from the theory of ordinary differential equations that there are two possible types of bifurcations[14] in eqs 11 and 13. The stable focus (SF) may become an unstable one (UF) due to the supercritical or subcritical Hopf bifurcations. It follows from the linear stability theory that the stable focus becomes an unstable one at

$$b = b_{cr} = \frac{1 + p_0}{b_1}[b_1^2(1 + p_0)(a_3 - s_0^{-2}) - a_2] \tag{18}$$

In the case of the supercritical Hopf bifurcation, a stable limit cycle (SLC) with a "radius" growing from zero appears if b decreases below b_{cr}. For the subcritical Hopf bifurcation, the radius of an unstable limit cycle (ULC) shrinks to zero at $b = b_{cr}$, and below this value, the UF is surrounded by the SLC. Which of these two bifurcations occurs depends on the sign of the first focus number.[12−14] To ensure the appearance of the subcritical Hopf bifurcation, the following values of the parameters have been chosen: $a_1 = a_2 = 0.005$, $a_3 = 250$, $b_1 = 0.0026$. For these values, the coordinates of the stationary state are $s_0 = 0.48$ and $p_0 = 2.124\,837\,248$. At these values, the first focus number is negative, and for values of $b \in (b_{cr},b_s)$, the SF coexists with the SLC, where $b_{cr} = 0.227\,501\,800$ and $b_s = 0.425\,42$. The last value has been determined numerically. Note that, in the above range of b, oscillations can be observed if the initial values of s and p are positioned outside of the ULC. For initial values of the reagents inside the ULC, the system evolves to the SF.

Let us now consider a one-dimensional (1D) bounded system of the length L'. We assume that the diffusion coefficients of the catalysts and their complexes can be neglected in comparison with the diffusion coefficients of the reactant (D_S) and the product (D_P). This assumption is fulfilled in experiments if the catalysts and their complexes are immobilized. Then, changes of the concentrations of s and p in the 1D system can be described by two nonlinear parabolic partial differential equations, which in dimensionless variables have the following form:

$$\frac{\partial s(x,t)}{\partial t} - \frac{\partial^2 s(x,t)}{\partial x^2} = a_1 - a_2s - \frac{s}{(1 + s + a_3s^2)(1 + p)} \tag{19}$$

$$\frac{\partial p(x,t)}{\partial t} - D\frac{\partial^2 p(x,t)}{\partial x^2} = b\left(\frac{s}{(1 + s + a_3s^2)(1 + p)} - b_1\right) \tag{20}$$

where $x = \sqrt{k_3E_0/(D_SK_m)}x'$ is the dimensionless spatial coordinate (x' is the coordinate in a physical one-dimensional space) and $D = D_P/D_S$. In numerical calculations, we assume that the diffusion coefficients of the reactant and the product are identical ($D = 1$).

Let us consider the initial-boundary (Fourier) problem with the zero flux (Neumann) boundary conditions

$$\frac{\partial s}{\partial x}(0,t) = \frac{\partial s}{\partial x}(L,t) = \frac{\partial p}{\partial x}(0,t) = \frac{\partial p}{\partial x}(L,t) = 0 \tag{21}$$

and the following initial conditions:

$$s(x,0) = s^*, \quad p(x,0) = p^* \quad \text{for} \quad x \in [0,l^*] \tag{22}$$

$$s(x,0) = s_0, \quad p(x,0) = p_0 \quad \text{for} \quad x \in (l^*,L] \tag{23}$$

where s^* and p^* belong to the basin of attraction of the SLC.

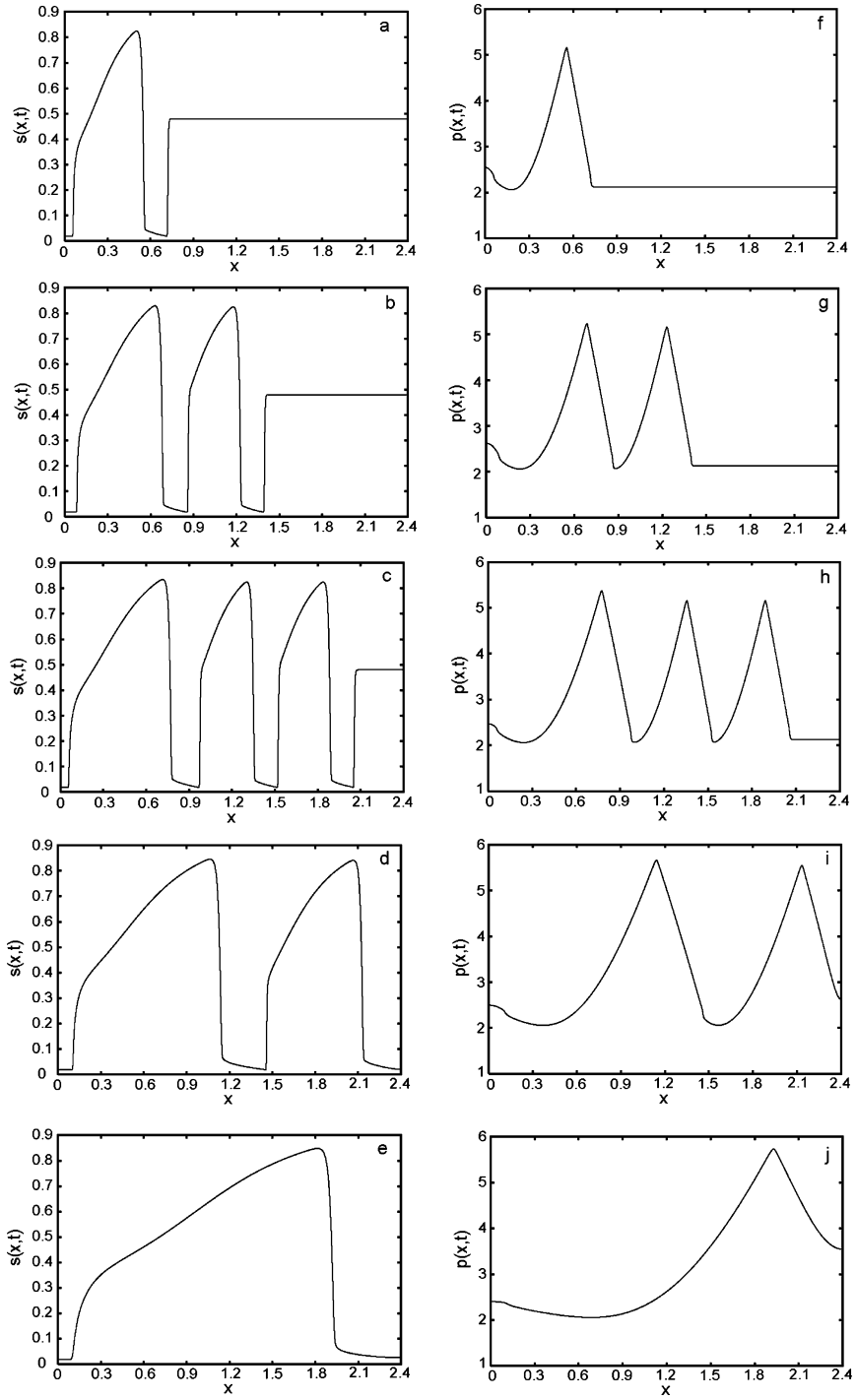

Figure 2. Solutions to the system (eqs 19−23) for $b = 0.24$ with the remaining parameters the same as those in Figure 1 and $L = 2.4$, $s^* = 0.01$, $p^* = p_0$, and $l^* = 0.015$ at the following times: 23 000 (a and f), 45 000 (b and g), 66 500 (c and h), 261 500 (d and i), and 1 706 500 (e and j). d$t = 1.0$, and d$x = 0.0006$.

Below, we present the dependence of evolutions of initial excitations on the bifurcation parameter b for values of the remaining parameters given above.

3. Results

The bifurcation parameter b controls the positions of the ULC and the SLC on the phase plane (s,p). For b close to b_{cr}, the ULC is small and is positioned very close to the SF, whereas the SLC is far from the SF. With increasing b, the ULC nears the SLC. The ULC moves away from the SF, and the basin of attraction of SF increases. A sufficiently strong vector field around the SF can induce a bend of the part of $s(x,t)$ and $p(x,t)$ which is positioned inside the ULC. Therefore, the size of the basin of attraction of SF plays a crucial role in the evolution of this part of the initial excitation, and in consequence, it may qualitatively change the form of the impulses of excitation.

Equations 19−23 have been solved numerically for selected values of the bifurcation parameter using the Cranck−Nicholson scheme of the second order in respect to the spatial step (dx) for diffusion terms and the Runge−Kutta algorithm of the fourth order in respect to the time step (dt) for the kinetic terms.

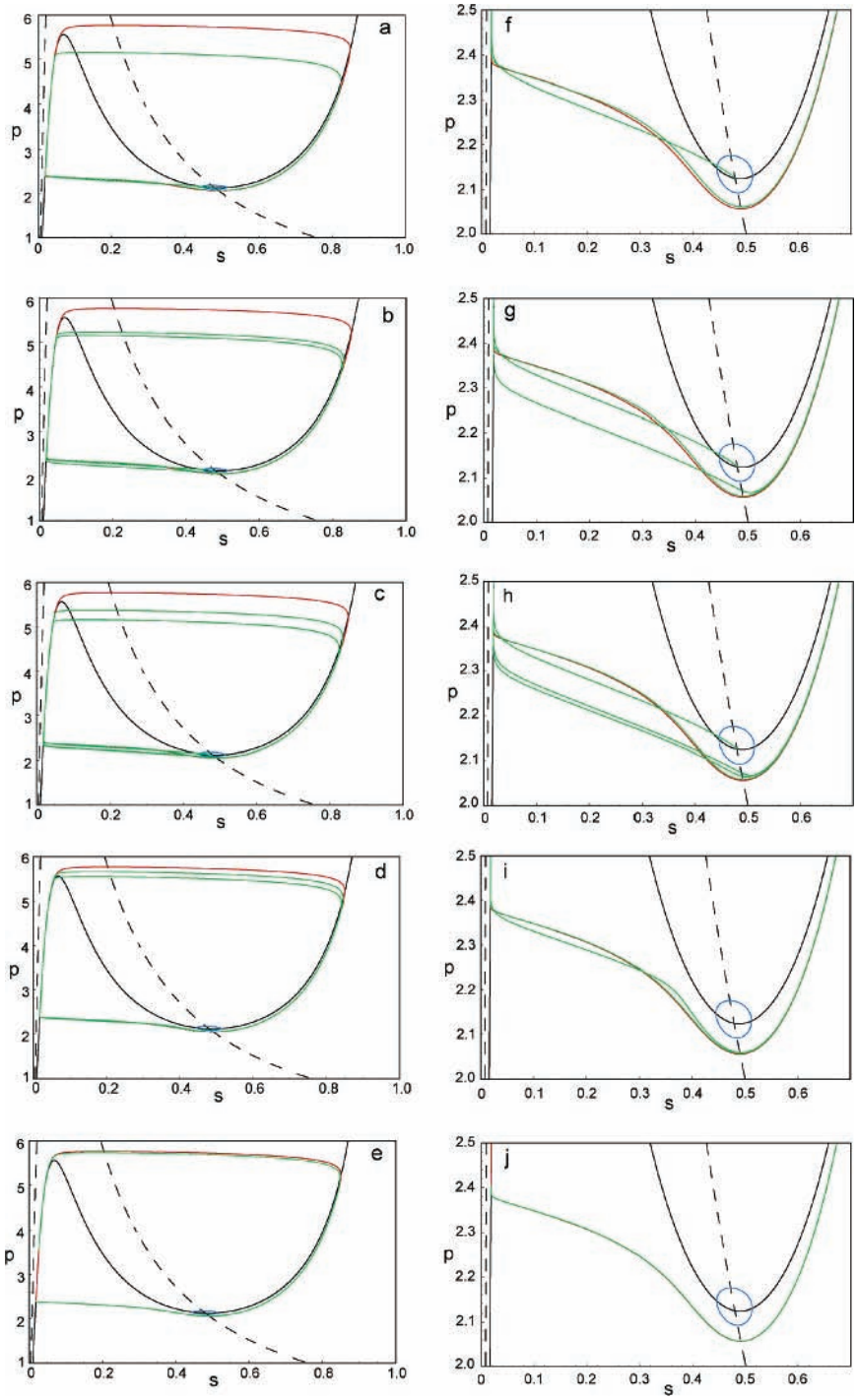

Figure 3. Parts a−e are projections of the distributions of $s(x,t)$ and $p(x,t)$ (green) on the phase plane corresponding to the solutions shown in Figure 2. Parts f−j show the projections of the backs of the impulses at the same times.

The initial excitation (eqs 22 and 23) with $s^* = 0.01$, $p^* = p_0$, and $l^* = 0.015$ for $L = 2.4$ at $b = 0.24$ causes the appearance of a sequence of traveling impulses of excitation. This value of b is slightly greater than b_{cr}, which means that the ULC is very small. The subsequent impulses move to the right boundary and disappear. The width of each impulse decreases during its spreading and attains asymptotic size sufficiently far from the interval of the initial excitation (see Figure 2). Each next impulse is initially wider than the previous one, because its back is formed later than the back of the previous impulse. Because the system is finite ($L < \infty$), the width of some new generated impulse becomes larger than L. The back of the impulse is not formed, and finally, the system oscillates homogeneously with the period characteristic for a SLC. Therefore, in a finite system, one can observe the generation of a finite sequence of impulses only. The sequential increasing of the initial widths of the impulses is illustrated in Figures 2 and 3. Figure 3 shows the distributions of s and p projected on the "phase plane". The subsequent impulses generate trajectories which are closer and closer to the SLC and asymptotically attain it. This limit corresponds to homogeneous oscillations of the reagent concentrations in the whole system. Of course, the correct phase space for the partial differential equations of the parabolic type has an infinite, uncountable dimension. However, projections

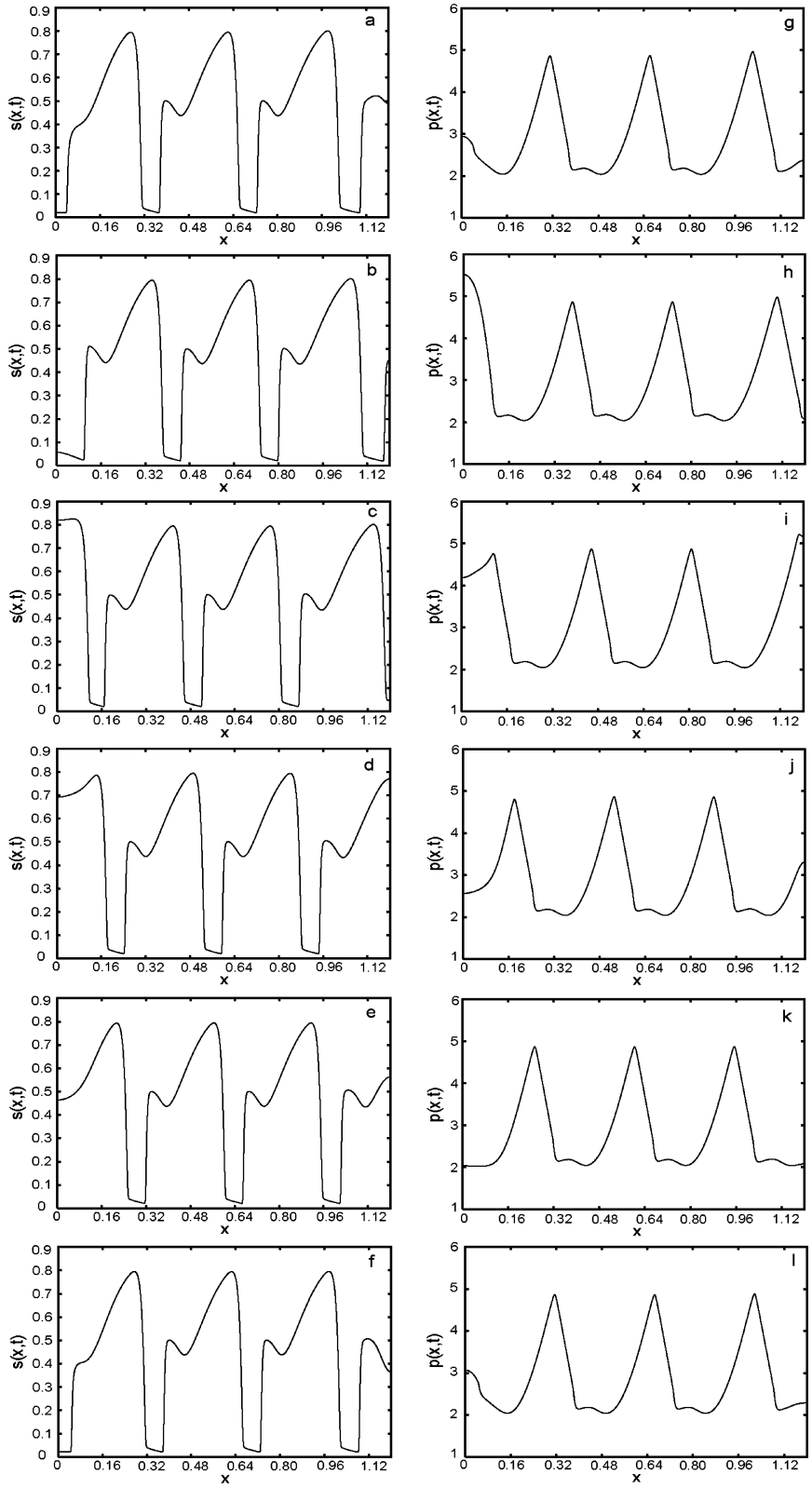

Figure 4. Solutions to the system (eqs 19−23) for $b = 0.4$, $L = 1.2$, and $l^* = 0.01$ at the following times: 102 000 (a and g), 105 000 (b and h), 108 000 (c and i), 111 000 (d and j), 114 000 (e and k), and 116 500 (f and l). The values of s^* and p^* are the same as those in Figure 2. $dt = 1.0$, and $dx = 0.0004$.

of the distributions of s and p on the phase plane (s,p) are helpful for our qualitative explanations.

It is noteworthy that in an infinite system there is no limit for the widths of the generated impulses. Therefore, different from the finite system, in infinite systems, an infinite sequence of impulses will be generated.

For larger values of b, the initial excitation induces the generation of impulses with concentration profiles shown in

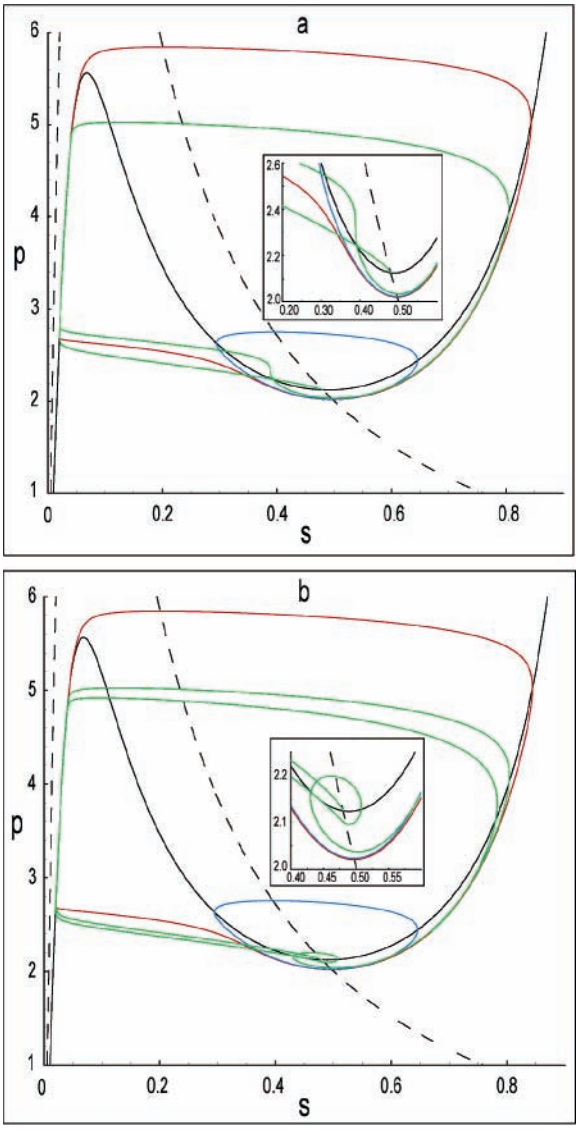

Figure 5. Projections of $s(x,t)$ and $p(x,t)$ (green) corresponding to solutions to the system (eqs 19−23) for $b = 0.4$ and $L = 0.8$. The formation of a minimum (between the front and the back) on the distribution of the reactant is seen in part a at $t = 15\,625$ as a bend in the inset. The formation of a maximum (between the back and the front) on the distribution of the product is seen in part b at $t = 22\,500$ as a loop in the inset. The values of s^*, p^*, l^*, dt, and dx are the same as those in Figure 4.

Figure 4. The impulse of $s(x,t)$ has a small local minimum between the front and the back, whereas the impulse of $p(x,t)$ has a corresponding small maximum. The appearance of these extremes can be explained by the qualitative analysis of the projections of the concentration distributions on the phase plane (s,p). The back of the impulse is partially positioned inside the ULC, where its further evolution is governed by the vector field around the SF (see Figure 5a). This part of the trajectory forms a bend, which in further evolution forms a loop (see Figure 5b). The formation of the bend on the projection means that a local minimum appears between the front and the back of the impulse of $s(x,t)$. Further evolution leads to the formation of a loop. This means that, beside the local minimum in $s(x,t)$, a local maximum appears between the back and the front in $p(x,t)$ (see Figure 4).

For values of b near b_s, where the ULC is close to the SLC, for a sufficiently small width of excitation l^*, we can observe only a single impulse traveling to the right boundary (see Figure 6), and then, the distributions of the reagents return to their stationary values. However, a finite number of impulses appears for the same value of b but greater values of l^*. The number of the impulses increases by one with l^*. Figure 7 shows the generation of four traveling impulses. The length of excitation above which the nonsustained wave source appears increases with the value b.

It follows from our numerical calculations that the period of oscillations observed at the point $x = x_1$, where the traveling impulses have their asymptotic form, is slightly greater than that for homogeneous oscillations. For example, for $b = 0.4$, it is equal to 14 348 (in arbitrary time units), whereas the homogeneous oscillations at the same value of b have a period equal to 14 029. The period of oscillations observed at $x = x_1$ does not depend on the initial conditions (eqs 22 and 23) but only on the parameters.

It is evident that, in order to create the impulses, one must initially excite a sufficiently large interval. Otherwise, the diffusion will disperse the initial excitation and the impulse will not be formed. Moreover, we have checked that initial excitations with (s^*,p^*) placed on the left lower horizontal part of the SLC ($s \in (0.01,0.3)$) induce wave sources on the shortest intervals l^*. Such initial excitation forms the back of the impulse, which is not dispersed by the diffusion. The back starts to run to the right boundary almost immediately. Increasing l^* for these values of (s^*,p^*) causes the first impulse to be formed at a greater distance from the left boundary. However, this distance slowly decreases for subsequent impulses. If (s^*,p^*) is situated on the vertical parts of the SLC, then longer intervals l^* are needed to initiate the sources. For (s^*,p^*) placed on the upper part of the SLC, wave sources are formed only for relatively large l^*. In these cases, the distributions of s and p in $[0, l^*)$ evolve almost homogeneously to the left lower part of the SLC, where the formation of the back of the traveling impulse begins. Note that the period of oscillations observed at a sufficiently large distance from the left boundary, where the traveling impulses have their asymptotic form, does not depend on the width of the initial excitation l^*. This property allows one to predict the interaction of various sources generated in the same system. Many sources may coexist in the system, because each of them generates traveling impulses with the same frequency. However, the place where the impulses from different wave sources meet depends on the lengths of the left (l_l^*) and the right (l_r^*) excitations with values of s_l^*, p_l^*, s_r^*, and p_r^*. The solutions to eqs 19−21 for the initial excitations in the following form:

$$s(x,0) = s_l^*, \quad p(x,0) = p_l^* \quad \text{for} \quad x \in [0,l_l^*] \tag{24}$$

$$s(x,0) = s_r^*, \quad p(x,0) = p_r^* \quad \text{for} \quad x \in [L - l_r^*,L] \tag{25}$$

$$s(x,0) = s_0, \quad p(x,0) = p_0 \quad \text{for} \quad x \in (l_l^*,l_r^*) \tag{26}$$

where $L = 2.0$, $l_l^* = 0.0125$, $l_r^* = 1.0$, $s_l^* = s_r^* = 0.01$, $p_l^* = p_r^* = p_0$, are shown in Figure 8. If $s_l^* = s_r^*$ and $p_l^* = p_r^*$, then the meeting point is shifted to the source which has been initialized on the shorter interval. This point is motionless, and for the case shown in Figure 8, it is equal to ≈0.8. If $l_l^* = l_r^*$ but $s_l^* \neq s_r^*$ or $p_l^* \neq p_r^*$, then the meeting point is shifted to the source whose back was formed earlier.

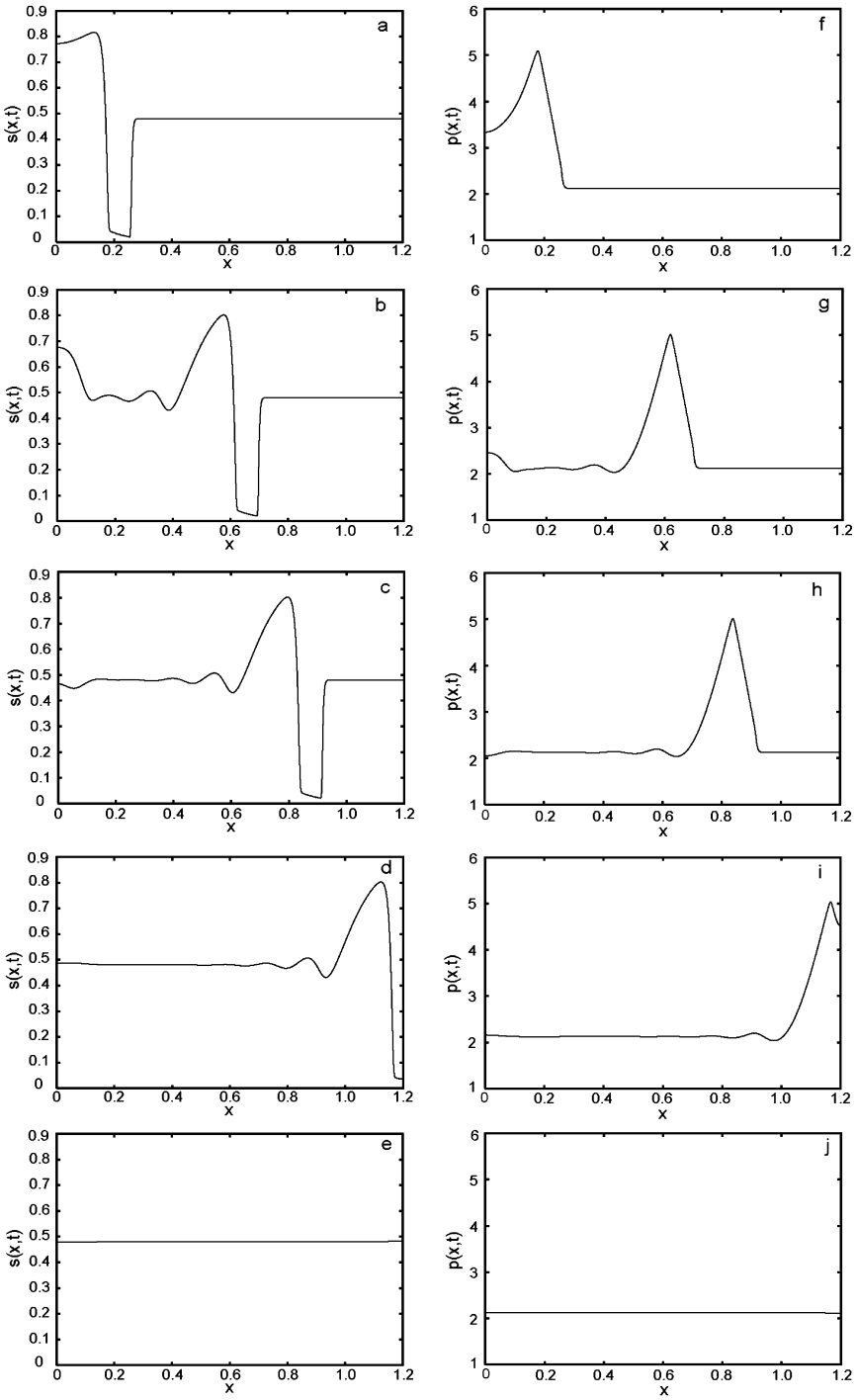

Figure 6. Solutions to the system (eqs 19−23) for $b = 0.41$, $L = 1.2$, and $l^* = 0.04$ at the following times: 8000 (a and f), 24 000 (b and g), 32 000 (c and h), 40 000 (d and i), and 80 000 (e and j). The values of s^*, p^*, dt, and dx are the same as those in Figure 4.

4. Discussion

The chemical system described in this paper is one of the simplest models in which the subcritical Hopf bifurcation is possible. It consists of nine elementary reactions excluding autocatalytic steps. There are well-known other two-variable chemical models, like the Oregonator,[15] in which the subcritical Hopf bifurcation is also possible. However, they were obtained from chemical schemes with a dozen or more variables.[16] There are many enzymes which are inhibited by an excess of their reactants and products. Examples include invertase inhibited by sucrose (reactant) and by fructose and glucose (products), xantine oxidase inhibited by xantine (reactant) and ureate (product), acetylcholinesterase inhibited by acetylcholine and choline, and many others.[17,18] One can expect that, under appropriate experimental conditions, the reactions with these enzymes immobilized in a 2D continuously fed unstirred reactor (CFUR) may generate the wave sources described in the present paper.

Our two-variable model should be treated as the minimal one in which the sources of waves described in this paper may appear. We want to stress that the wave sources described above may be observed in all chemical systems in which the SF is

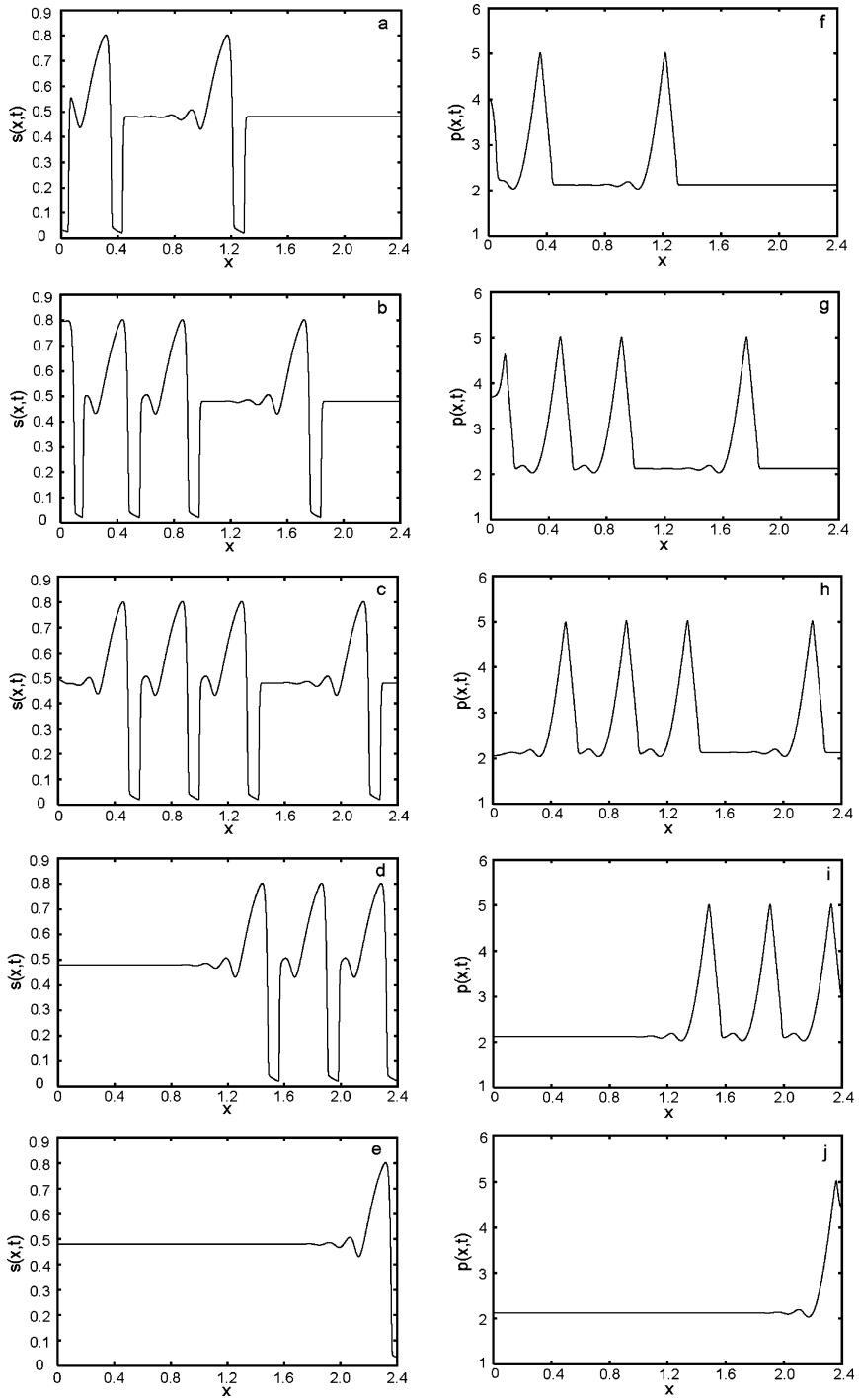

Figure 7. Solutions to the system (eqs 19−23) for $b = 0.41$, $L = 2.4$, and $l^* = 0.09$ at the following times: 44 000 (a and f), 64 000 (b and g), 80 000 (c and h), 116 000 (d and i), and 148 000 (e and j). The values of s^*, p^*, dt, and dx are the same as those in Figure 6.

surrounded by the ULC and SLC regardless of the dimension of the corresponding phase space. Real chemical systems are known such as the chlorite−iodide oscillator[19] and the peroxidase−oxidase reaction[20] in which the coexistence of the stable stationary state surrounded by a SLC has been observed. These systems are described models with more than two variables, but they are also possible candidates in which the wave sources can be observed. It is noteworthy that in our concept of the generation of wave sources not the number of variables in a system dynamics but the existence of the subcritical Hopf bifurcation is crucial. The generation of sources of waves in the two-variable system exhibiting the subcritical Hopf bifurcation was reported some years ago.[21] These sources have properties similar to one of the types of sources described above for the case when the basin of attraction of SF is small. They also have periods of generation close to the period of homogeneous oscillations.

We want to stress that the wave sources described in the present paper have different properties from the leading centers or pacemakers mentioned in the Introduction. The wave sources described in this paper appear as a result of perturbations of the stationary state, whereas leading centers have been observed from perturbations of stationary states as well as by perturbations of homogeneous periodic oscillations. Also, pacemakers may

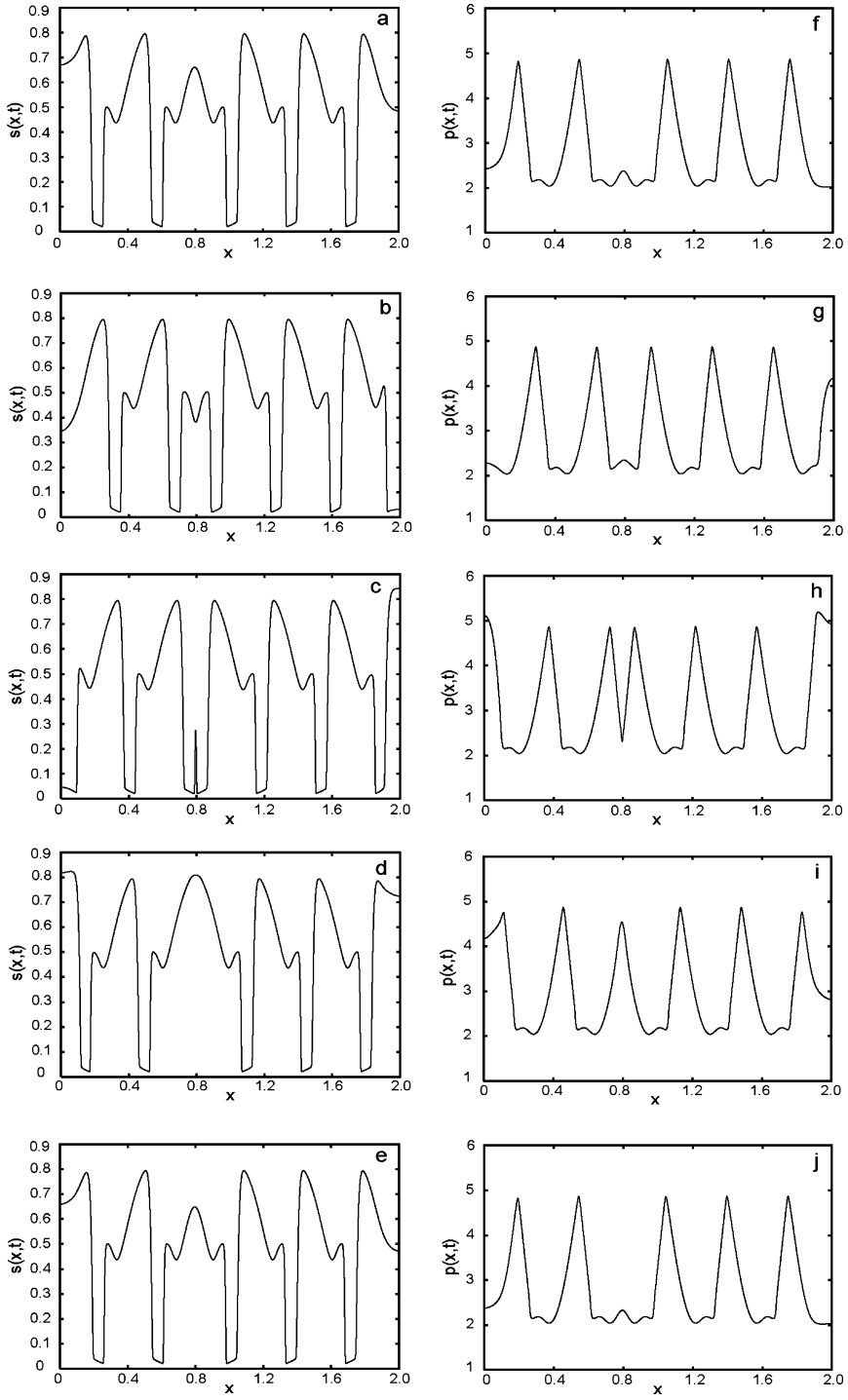

Figure 8. Solutions to the system (eqs 19−23) with initial conditions (eqs 24−26) where $L = 2.0$, $l_l^* = 0.0125$, $l_r^* = 1.0$, $s_l^* = s_r^* = 0.01$, and $p_l^* = p_r^* = p_0$ at the following times: 1 015 500 (a and f), 1 019 500 (b and g), 1 023 000 (c and h), 1 026 500 (d and i), and 1 030 000 (e and j). $dt = 1.0$, and $dx = 0.0005$.

appear in systems with homogeneous stable stationary states as well as in systems with homogeneous stable oscillations. Moreover, to the best of our knowledge, all sources of waves known so far generate impulses without a minimum between their fronts and backs, whereas impulses with a minimum between the fronts and backs may appear in our system as well as in other systems exhibiting the subcritical Hopf bifurcation.

In our deterministic model, the wave sources appear due to well-defined initial conditions. However, in real systems exhibiting the subcritical Hopf bifurcation, they can appear spontaneously due to internal fluctuations.

References and Notes

(1) Zaikin, A. N.; Zhabotinsky, A. M. *Nature* **1970**, *225*, 535.
(2) Zhabotinsky, A. M.; Zaikin, A. N. *J. Theor. Biol.* **1973**, *40*, 45.
(3) Kurin-Csörgei, K.; Szalai, I.; Körös, E. *React. Kinet. Catal. Lett.* **1995**, *54*, 217.
(4) Orbán, M.; Kurin-Csörgei, K.; Zhabotinsky, A. M.; Epstein, I. R. *J. Am. Chem. Soc.* **1998**, *120*, 1146.
(5) Orbán, M. *J. Am. Chem. Soc.* **1980**, *102*, 4311.
(6) De Kepper, P.; Epstein, I. R.; Kustin, K.; Orbán, M. *J. Phys. Chem.* **1982**, *86*, 170.
(7) Jakubith, S.; Rotermund, H. H.; Engel, W.; von Oertzen, A.; Ertl, G. *Phys. Rev. Lett.* **1990**, *65*, 3013.
(8) Tyson, J. J.; Fife, P. C. *J. Chem. Phys.* **1980**, *73*, 2224.

(9) Kawczyński, A. L. *Pol. J. Chem.* **1986**, *60*, 223.
(10) Zaikin, A. N.; Kawczyński, A. L. *J. Non-Equilib. Thermodyn.* **1977**, *2*, 39.
(11) Tikhonov, A. N. *Mater. Sb., Statni Vyzk. Ustav Mater.* **1952**, *31*, 575.
(12) Bautin, N. N. *Behaviour of Dynamic Systems in the Neighbourhood of Boundaries of Stability*; State Tech. Publ.: Moscow, 1949.
(13) Andronov, A. A.; Leontovich, E. A.; Gordon, I. I.; Maier, A. G. *Bifurcation Theory of Dynamics Systems on the Plane*; Wiley: New York, 1972.
(14) Górski, J.; Kawczyński, A. L. *J. Non-Equilib. Thermodyn.* **1979**, *4*, 295.
(15) Field, R. J.; Noyes, R. M. *J. Chem. Phys.* **1974**, *60*, 1877.
(16) *Oscillations and Traveling Waves in Chemical Systems*; Field, R. J., Burger, M., Eds.; Wiley: New York, 1985.
(17) Sel'kov, E. E. On the Possibility of Appearing of Oscillations in the Enzymatic Reactions with Feedback. In *Oscillatory Processes in Biological and Chemical Systems*; Sci. Publ.: Moscow, 1967; Vol. 1, p 93.
(18) Golbeter, A. *Biochemical Oscillations and Cellular Rhythms*; Cambridge University Press: Cambridge, U.K., 1996.
(19) Dateo, C. E.; Orban, M.; De Kepper, P.; Epstein, I. R. *J. Am. Chem. Soc.* **1982**, *104*, 504.
(20) Aguda, B. D.; Frisch, L. H.; Olsen, L. F. *J. Am. Chem. Soc.* **1990**, *112*, 6652.
(21) Ohta, T.; Hayase, Y.; Kobayashi, R. *Phys. Rev. E* **1996**, *54*, 6074.